ACS Macro Letters

Letter

pubs.acs.org/macroletters

Confinement Induced Preferential Orientation of Crystals and Enhancement of Properties in Ferroelectric Polymer Nanowires

Yangjiang Wu,[†] Qingzhao Gu,[†] Guangzhu Ding,[†] Fuqiang Tong,[‡] Zhijun Hu,*[,†] and Alain M. Jonas[§]

[†]Center for Soft Condensed Matter Physics and Interdisciplinary Research, Soochow University, Suzhou 215006, China

[‡]Department of Physics and Jiangsu Key Laboratory of Thin Films, Soochow University, Suzhou 215006, China

[§]Institue of Condensed Matter and Nanosciences − Bio and Soft Matter (IMCN/BSMA), Université Catholique de Louvain, Croix du Sud 1/L7.04.02, 1348 Louvain-la-Neuve, Belgium

Supporting Information

ABSTRACT: The physical properties of polymers strongly depend on the molecular or supermolecular order and orientation. Here we demonstrate the preferential orientation of lamellar crystals and the enhancement of ferro/piezoelectric properties in individual poly(vinylidene fluoride-*co*-trifluoroethylene) (P(VDF-TrFE)) nanowires fabricated from anodic alumina oxide (AAO) templates. The crystallographic *a* axis of P(VDF-TrFE) was found to be aligned along the long axis of nanowires due to geometrical confinement and grapho-expitaxial crystals growth. The alignment of lamellar crystals in P(VDF-TrFE) nanowires and enhancement of crystallization translated into improved ferro/piezoelectric properties such as lower coercive field and higher piezoelectric coefficient, testified by piezoresponse force microscopy images and piezoresponse hysteresis loops.

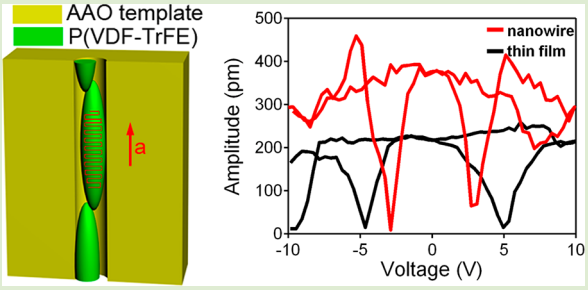

Arrays of polymer nanostructures have attracted tremendous interest because they offer a promising route to novel devices in diverse fields such as photonics,[1] electronics,[2] sensing,[3] adhesion,[4] and biotechnology.[5] In the microelectronics industry, highly ordered arrays of polymer nanostructures are also required for temporal templates of nanofabrication.[6] While the processing and device integration of polymer nanostructures has progressed rapidly over the past decade, the size-dependent physical behaviors and properties are of great importance and interest in both fundamental and application aspects. As in many geometrically constrained materials, studies on the size effects in polymer nanostructures have revealed that various physical behaviors such as chain dynamics[7] and crystallization[8] can deviate significantly from their bulk counterparts.

Among the various functional polymer materials, ferroelectric polymers, such as poly(vinylidene fluoride) (PVDF) and its copolymers with trifluoroethylene (P(VDF-TrFE)), are attractive because they exhibit an excellent solution processability, a low processing temperature, excellent ferroelectric and electromechanical properties.[9] P(VDF-TrFE) is even more attractive because it crystallizes in a stable ferroelectric β phase without the additional processing steps required for the homopolymer PVDF for which mechanical stretching and electric poling have to be applied. Ferroelectric P(VDF-TrFE) has recently been used for a variety of piezoelectric and pyroelectric devices,[10] nonvolatile memories,[11−14] organic solar cells,[15,16] and for tuning magnetic or ferromagnetic properties.[17,18] The importance of arrays of ferroelectric polymer nanostructures has also recently been recognized with the increasing demand for development and miniaturization of novel organic electronic devices such as high density nonvolatile memories, nanogenerators, and sensors.[2,19−21]

Arrays of P(VDF-TrFE) nanostructures are typically fabricated by nanoimprinting with a mold[2,22,23] and template-assisted infiltration.[24−29] Importantly, preferential orientation of lamellar crystals due to geometrical confinement and grapho-epitaxial crystal growth has been found during the fabrication of ferroelectric polymer nanostructures[2,26] In addition, the oriented crystals in ferroelectric polymer nanostructures can give rise to enhancement in ferroelectric properties, such as well-defined uniform switching behavior and lower coercive field, as we found in P(VDF-TrFE) nanostructures with a low aspect ratio achieved by nanoimprinting.[2] Among nanostructures, one-dimensional nanowires of high aspect ratio are favorable to study size effects on structure and properties. However, structure−property relationships still remain largely unknown in ferroelectric nanowires.

We report here on the preferential crystal orientation and the resulting ferroelectric and piezoelectric properties of P(VDF-TrFE) nanowires. The P(VDF-TrFE) nanowires were prepared by solution wetting of anodic alumina oxide (AAO) templates with nominal pore diameters ~40, 60, and 80 nm, and subsequently annealed in the paraelectric phase at 135 °C for 6

Received: April 25, 2013
Accepted: May 30, 2013
Published: June 3, 2013

   dx.doi.org/10.1021/mz400208k | *ACS Macro Lett.* 2013, 2, 535−538

h. The continuous layer of P(VDF-TrFE) remaining on the surface of AAO was removed by scratching with a blade. Figure 1a shows a scanning electron microscopy (SEM) image of the

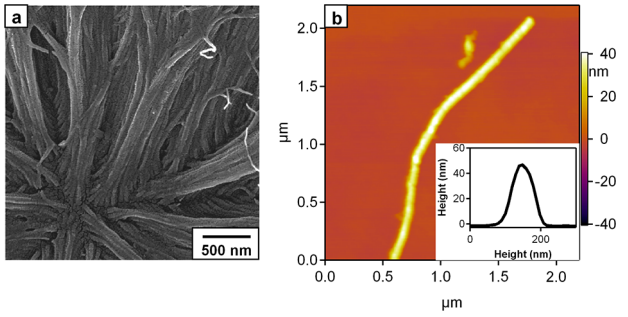

Figure 1. Morphology of P(VDF-TrFE) nanowire arrays fabricated by infilling an AAO template and subsequent annealing. (a) SEM image of nanowires after template removal. (b) AFM topography image of a single nanowire collected on a silicon substrate.

fabricated P(VDF-TrFE) nanowires of about 60 nm nominal diameter, after release from the AAO template, indicating proper nanowire fabrication. The length of the nanowires is similar to the depth of the nanopores in the AAO templates. Atomic force microscopy (AFM) topography images of nanowires dispersed on a silicon wafer from ethanol solution show that the nanowire radial dimensions are in accordance with the nominal channel width of the used AAO templates (average diameters of 40, 60, and 80 nm; Figure 1b). The nanowires may be bended or shortened when dispersed on the substrates.

Enhanced crystallization and preferential orientation of crystals have been found previously in P(VDF-TrFE) nanostructures achieved by nanoimprinting[2] and template-assisted infiltration.[25,26] To verify the crystal structure and preferential orientation of crystals in our P(VDF-TrFE) nanowires, wide-angle X-ray diffraction (WAXD) in reflection mode was first performed on the P(VDF-TrFE) nanowires kept in AAO templates of various pore diameter. Comparisons were also made with bulk samples annealed in the same conditions as the nanowires (Figure 2a). In such a configuration, the scattering vector is perpendicular to the template surface and thus only lattice planes oriented parallel to the surface of the template contribute to the intensity of a Bragg reflection. Several diffraction peaks at 19.9° (200, 110), 35.2° (001, 020, 310), and 40.8° (111, 201, 220, 400) can be observed in the bulk samples, comparable to prior reports.[30,31] Strikingly, the diffraction peaks at 35.2 and 40.8° are practically absent for the nanowires in AAO templates, suggesting preferential orientation of the (200) or (110) planes in the P(VDF-TrFE) nanowires. These results are in good agreement with previous reports.[25,26]

However, because two Bragg reflections (200, 110) overlap at 19.9°, essentially owing to the pseudohexagonal nature of the crystal structure of the ferroelectric phase of P(VDF-TrFE),[30,31] different crystal settings are still compatible with the diffraction pattern of the nanostructures. To precisely study the orientation of P(VDF-TrFE) crystals in the nanowires, selected area electron diffraction (SAED) from transmission electron microscopy (TEM) was analyzed on single P(VDF-TrFE) nanowires released from AAO templates and floated onto TEM grids coated with amorphous carbon. Typically, two different sets of SAED patterns were observed from different nanowires (Figure 2b,c). At first sight, all the SAED patterns present very oriented, single crystal-like reflections, confirming the high degree of structural order of the chain packing in the nanowires. Further analysis of the patterns reveals that all the reflections along the long axes of P(VDF-TrFE) nanowires can be indexed to the (h00) reciprocal lattice section of the ferroelectric β phase, indicating the preferential orientation of the crystallographic *a* axis along the nanowires. Correspondingly, the polar *b* axis is perpendicular to the long axes of P(VDF-TrFE) nanowires, being tilted or parallel to the substrate in Figure 2b and 2c, respectively. This indicates that the crystallographic *b* axis is randomly oriented with respect to the substrate, which is logical since the cross-section of the nanowires is circular and there is no reason to favor one specific orientation of this axis. This shows that the crystal lamellae align with their basal planes parallel to the pore axis. which contrasts with the observations of Lutkenhaus et al.[26] who reported that P(VDF-TrFE) lamellae are perpendicular to the pore axis when crystallized in AAO templates. This difference of orientation is probably related to the different thermal treatments applied to crystallize P(VDF-TrFE), because in this previous report the samples were crystallized from the molten state. We and others have recently shown that the orientation of P(VDF-TrFE) crystalline lamellae in ultrathin films strongly depends on the details of the thermal treatment applied during crystallization.[32] A similar effect is probably at work here.

Because single-crystal-like structures and preferential axial orientation of the crystallographic *a* axis have been found, it is crucial to probe the domain structure and switching behavior of the P(VDF-TrFE) nanowires. Piezoresponse force microscopy (PFM) provides a powerful means to investigate the ferroelectric properties at the nanoscale and was applied in recent years to study the ferroelectricity of P(VDF-TrFE) thin films and nanomesas.[33,34] A low alternating voltage (1 V), which is expected to be much lower than the coercive voltage of the nanowires, thus, preventing inadvertent polarization switching, was applied to the conductive cantilever to excite the

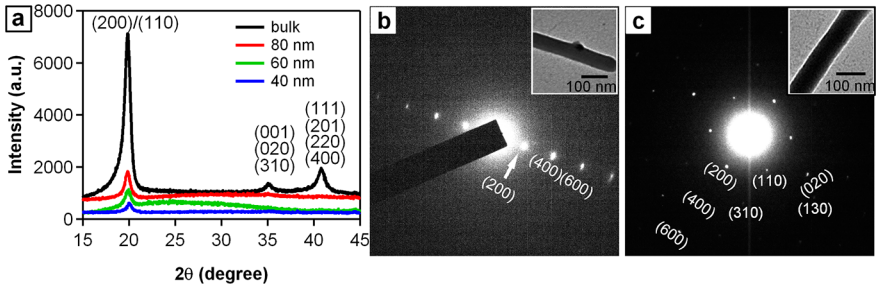

Figure 2. Structural study of P(VDF-TrFE) nanowires by WAXD (a) and SAED (b, c).

dx.doi.org/10.1021/mz400208k | *ACS Macro Lett.* 2013, 2, 535−538

piezoelectric vibration of the sample. Figure 3 shows the resulting piezoresponse amplitude and phase images of isolated

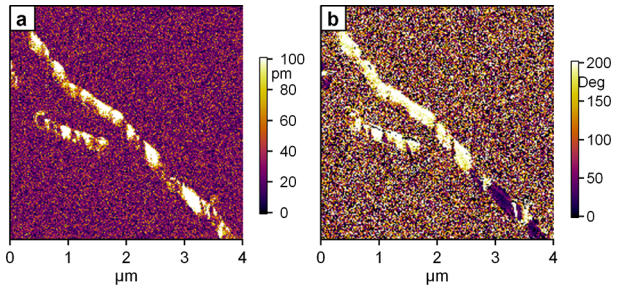

Figure 3. PFM images of isolated P(VDF-TrFE) nanowires, measured with an alternating driving voltage of 1.0 V. (a) Amplitude image and (b) phase image presented with respective color scale bars in picometers or degrees.

P(VDF-TrFE) nanowires, where the amplitude and phase provide information on the piezoelectric coefficient and on the direction of the local polarization, respectively. The analyzed P(VDF-TrFE) nanowires, irrespective of their diameters, show positive domains (white contrast) in the amplitude signal, a clear indication of a piezoresponse in the nanowires resulting from out-of-plane polarization. The ferroelectric domains in each individual nanowire essentially extend over the full diameters. Along the nanowires, domain walls appear as narrow dark lines with lower amplitude signals. Associated with the out-of-plane polarization, the piezoresponse phase image of the nanowires shows 180° contrast between domains, as shown in Figure 3b. The phase indicates whether the vertical projection of the polar *b* axis of P(VDF-TrFE) nanowires points either upward or downward, which depends on the specific orientation of the *b* axis that samples all possible orientations compatible with the *a* axis aligned along the nanowire axis, in agreement with our conclusions from SAED.

To quantify the switching and piezoelectric properties of the P(VDF-TrFE) nanowires, piezoresponse hysteresis loops (PHLs) composed of phase-voltage and amplitude-voltage loops were measured with PFM by adding a sequence of dc bias in triangle sawtooth form to the ac driving voltage. To minimize the contribution of electrostatic interactions, the PHLs were measured in the "off" state at each step, that is, the dc voltage was programmed back to zero between each step of dc bias. Almost 180° phase contrast is observed in phase-voltage PHLs of all P(VDF-TrFE) nanowires, as shown in Figure 4a, a clear indication of polarization switching. In addition, the switching voltage increases with increasing diameter of the (PVDF-TrFE) nanowires (Figure S1 in the

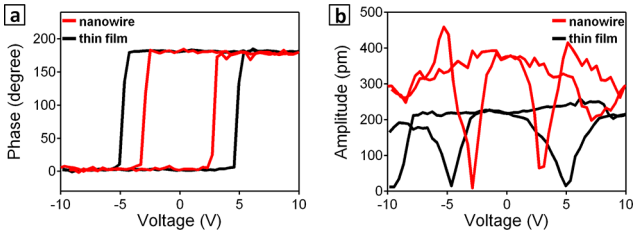

Figure 4. PFM (a) phase-voltage and (b) amplitude-voltage hysteresis loops in the "off" state of a P(VDF-TrFE) nanowire of 60 nm diameter, compared to the ones of a uniform thin film of 60 nm thickness.

Supporting Information). By simply calculating the coercive field by dividing the switching voltage by the diameters of the nanowires, the coercive field for P(VDF-TrFE) nanowires of different diameters in the range of 40−80 nm was found to be similar, about 40 MV/m. This is significantly lower than the coercive field of the thin film (∼80 MV/m) and bulk[31] (∼50 MV/m) samples. The lower coercive field may result from the enhancement of crystallinity in *β* phase in P(VDF-TrFE) nanowires and to the increased fraction of favorably aligned crystals when the chain axis is only allowed to rotate along the nanowire axis, compared to the film samples wherein crystals adopt random orientations.[30,31] Indeed, the efficient part of the torque exerted by the vertical electric field on a dipole moment of the P(VDF-TrFE) chains is the projection of the torque on the chain axis; this projection depends on the angle between the field and the dipole moment and on the angle between the chain axis and the field. Therefore, different distributions of crystal orientations lead to different average values of the torque, and as a result different coercive fields. A similar effect was reported by us for nanoimprinted samples;[2] in this specific case, the *c* axis was in-plane, which resulted in optimal coupling between the field and the dipole moments. For the case of the nanowires of the present paper, the situation is intermediate.

Associated with phase reversal, butterfly shaped amplitude-voltage loops that saturate at a relatively high voltage are observed in the P(VDF-TrFE) nanowires. To compare the piezoelectric coefficients of P(VDF-TrFE) nanowires with the ones of thin films, only the amplitude-voltage loop of nanowires of 60 nm diameter is given in Figure 4b, along with a loop measured from a uniform thin film of 60 nm thickness annealed in the same conditions. The amplitude from the nanowires is much higher than that from the uniform thin film. We estimate the piezoelectric coefficient d_{33} using the equation $A = d_{33}V_{ac}Q$, where A is the amplitude, V_{ac} is the driving voltage, and Q is the quality factor (Q = 10 in our experiments). The d_{33} of the P(VDF-TrFE) nanowires with a diameter of 60 nm is in the range of 25−45 pm/V, much larger than the corresponding uniform thin films (16−23 pm/V). For P(VDF-TrFE) nanowires with other diameters, the piezoelectric coefficient d_{33} is also larger than that of the corresponding thin films with similar thickness (Figure S1 in the Supporting Information). Additionally, the d_{33} of the nanowires is larger than that of bulk samples (3−19 pm/V in 600−700 nm thick films), wherein crystals adopt random orientations.[23] This indicates that the piezoelectric properties of P(VDF-TrFE) are enhanced in the nanowires due to the enhanced crystallization and preferential orientation of *β* phase crystals.

We note here that the lower coercive field and higher piezoelectric coefficient were observed in all the measured (PVDF-TrFE) nanowires, in contrast with the random orientation of nanowires with respect to substrate as proved by SAED shown in Figure 2. This is probably due to the fact that there are charge-dipole interactions between the nanowires and the silicon substrate used for PFM measurement, leading to perpendicular orientation of polar *b* axis with respect to the substrate surface. For the nonpolar substrate, such as amorphous carbon used for TEM experiments, there is no specific interaction between the nanowires and substrate. The nanowires thus are randomly oriented on the substrate. The shapes of P(VDF-TrFE) nanowire's PHLs are also different from the observation of Choi et al.[29] who reported the macroscopic polarization-voltage hysteresis loops of nanowires and nanotubes along with the AAO templates in the direction

dx.doi.org/10.1021/mz400208k | *ACS Macro Lett.* 2013, 2, 535−538

of pore axis. In the case of macroscopic measurements, the loops were not saturated due to the existence of AAO templates and limited voltage.

In summary, the present work shows that ferroelectric P(VDF-TrFE) nanowires can be fabricated by solution infiltration in templates. The crystallization and preferential orientation of the ferroelectric β phase is enhanced due to the geometrical confinement and grapho-epitaxial crystal growth. The crystallographic *a* axis is aligned along the long axis of nanowires. The enhanced crystallization and preferential orientation of β phase translate into improved ferroelectric and piezoelectric properties such as lower coercive field and increased piezoelectric coefficient. These results suggest that ferroelectric P(VDF-TrFE) nanostructures can be suitably applied to the fabrication novel organic electronic or photonic devices.

■ ASSOCIATED CONTENT

Supporting Information

Detailed experimental procedure for the sample preparation, morphology, and structure characterization and ferro/piezoelectric properties. This material is available free of charge via the Internet at http://pubs.acs.org.

■ AUTHOR INFORMATION

Corresponding Author

*E-mail: zhijun.hu@suda.edu.cn.

Notes

The authors declare no competing financial interest.

■ ACKNOWLEDGMENTS

This work was supported by the National Science Foundation of China (Nos. 21074084, 91027040), the Natural Science Foundation of Jiangsu Province of China (No. BK2010213), and a Project Funded by the Priority Academic Program Development of Jiangsu Higher Education Institutions (PAPD). A.M.J. acknowledges financial support from the EU Program FP7/2007-2013 (MOMA, Agreement No. 248092), the Belgian Federal Science Policy (IAP P7/05), and the F.R.S.-FNRS. The authors thank Solvay Specialty Polymers for the gift of the P(VDF-TrFE) sample.

■ REFERENCES

(1) von Freymann, G.; Ledermann, A.; Thiel, M.; Staude, I.; Essig, S.; Busch, K.; Wegener, M. *Adv. Funct. Mater.* **2010**, *20*, 1038−1052.
(2) Hu, Z.; Tian, M.; Nysten, B.; Jonas, A. M. *Nat. Mater.* **2009**, *8*, 62−67.
(3) Dong, B.; Lu, N.; Zelsmann, M.; Kehagias, N.; Fucks, H.; Torres, C. M. S.; Chi, L. *Adv. Funct. Mater.* **2006**, *16*, 1937−1942.
(4) Jeong, H. E.; Lee, J.-H.; Kim, H. N.; Moon, S. H.; Suh, K. Y. *Proc. Natl. Acad. Sci. U.S.A.* **2009**, *106*, 5639−5644.
(5) Yang, M. T.; Sniadechi, N. J.; Chen, C. S. *Adv. Mater.* **2007**, *19*, 3119−3123.
(6) Bratton, D.; Yang, D.; Dai, J. Y.; Ober, C. K. *Polym. Adv. Technol.* **2006**, *17*, 94−103.
(7) Shin, K.; Obukhov, S.; Chen, J.-T.; Huh, J.; Hwang, Y.; Mok, S.; Dobriyal, P.; Thiyagarajan, P.; Russell, T. P. *Nat. Mater.* **2007**, *6*, 961−965.
(8) Loo, Y.-L.; Register, R. A.; Ryan, A. J. *Phys. Rev. Lett.* **2000**, *84*, 4120−4123.
(9) Furukawa, T. *Phase Transitions* **1989**, *18*, 143−211.
(10) Lovinger, A. J. *Science* **1983**, *220*, 1115−1121.
(11) Naber, R. C. G.; Tanase, C.; Blom, P. W. M.; Gelinck, G. H.; Marsman, A. W.; Touwslager, F. J.; Setayesh, S.; de Leeuw, D. M. *Nat. Mater.* **2005**, *4*, 243−248.
(12) Asadi, K.; de Leeuw, D. M.; de Boer, B.; Blom, P. W. M. *Nat. Mater.* **2008**, *7*, 547−550.
(13) Das, S.; Appenzeller, J. *Nano Lett.* **2011**, *11*, 4003−4007.
(14) Khan, M. A.; Bhansali, U. S.; Alshareef, H. N. *Adv. Mater.* **2012**, *24*, 2165−2170.
(15) Yuan, Y.; Reece, T. J.; Sharma, P.; Poddar, S.; Ducharme, S.; Gruverman, A.; Yang, Y.; Huang, J. *Nat. Mater.* **2011**, *10*, 296−302.
(16) Yang, B.; Yuan, Y.; Sharma, P.; Poddar, S.; Korlacki, R.; Ducharme, S.; Gruverman, A.; Saraf, R.; Huang, J. *Adv. Mater.* **2012**, *24*, 1455−1460.
(17) Stolichnov, I.; Riester, S. W. E.; Trodahl, H. J.; Setter, N.; Rushforth, A. W.; Edmonds, K. W.; Campion, R. P.; Foxon, C. T.; Gallagher, B. L.; Jungwirth, T. *Nat. Mater.* **2008**, *7*, 464−467.
(18) Mardana, A.; Ducharme, S.; Adenwalla, S. *Nano Lett.* **2011**, *11*, 3862−3867.
(19) Ducharme, S.; Gruverman, A. *Nat. Mater.* **2009**, *8*, 9−10.
(20) Tripathi, A. K.; van Breemen, A. J. J. M.; Shen, J.; Gao, Q.; Ivan, M. G.; Reimann, K.; Meinders, E. R.; Gelinck, G. H. *Adv. Mater.* **2011**, *23*, 4146−4151.
(21) Kang, S. J.; Bae, I.; Shin, Y. J.; Park, Y. J.; Huh, J.; Park, S.-M.; Kim, H.-C.; Park, C. *Nano Lett.* **2011**, *11*, 138−144.
(22) Hong, C.-C.; Huang, S.-Y.; Shieh, J.; Chen, S.-H. *Macromolecules* **2012**, *45*, 1580−1586.
(23) Liu, Y.; Weiss, D. N.; Li, J. *ACS Nano* **2010**, *4*, 83−90.
(24) Serghei, A.; Lutkenhaus, J. L; Miranda, D. F.; McEnnis, K.; Kremer, F.; Russell, T. P. *Small* **2010**, *6*, 1822−1826.
(25) Oh, S.; Kim, Y.; Choi, Y.-Y.; Kim, D.; Choi, H.; No, K. *Adv. Mater.* **2012**, *24*, 5708−5712.
(26) Lutkenhaus, J. L.; McEnnis, K.; Serghei, A.; Russell, T. P. *Macromolecules* **2010**, *43*, 3844−3850.
(27) Li, X.; Lim, Y.-F.; Yao, K.; Tay, F. E. H.; Seah, K. H. *Chem. Mater.* **2013**, *25*, 524−529.
(28) Cauda, V.; Torre, B.; Falqui, A.; Canavese, G.; Stassi, S.; Bein, T.; Pizzi, M. *Chem. Mater.* **2012**, *24*, 4215−4221.
(29) Choi, K.; Lee, S. C.; Liang, Y.; Kim, K. J.; Lee, H. S. *Macromolecules* **2013**, *46*, 3067−3073.
(30) Bellet-Amalric, E.; Legrand, J. F. *Eur. Phys. J. B* **1998**, *3*, 225−236.
(31) Tashiro, K. In *Ferroelectric Polymers: Chemistry, Physics, and Applications*; Nalwa, H. S., Ed.; Dekker: New York, 1995; pp63−181.
(32) Park, Y. J.; Kang, S. J.; Park, C.; Kim, K. J.; Lee, H. S.; Lee, M. S.; Chung, U. I.; Park, I. J. *Appl. Phys. Lett.* **2006**, *88*, 242908.
(33) Sharma, P.; Reece, T. J.; Ducharme, S.; Gruverman, A. *Nano Lett.* **2011**, *11*, 1970−1975.
(34) Stolichnov, I.; Maksymovych, P.; Mikheev, E.; Kalinin, S. V.; Tagantsev, A. K.; Setter, N. *Phys. Rev. Lett.* **2012**, *108*, 027603.